

Total cross section measurements for electron scattering from dichloromethane

Cite as: J. Chem. Phys. **149**, 244304 (2018); <https://doi.org/10.1063/1.5080636>

Submitted: 10 November 2018 . Accepted: 05 December 2018 . Published Online: 26 December 2018

A. I. Lozano, L. Álvarez, F. Blanco , M. J. Brunger, and G. García 



View Online



Export Citation



CrossMark

ARTICLES YOU MAY BE INTERESTED IN

[Integral elastic, vibrational-excitation, electronic-state excitation, ionization, and total cross sections for electron scattering from para-benzoquinone](#)

The Journal of Chemical Physics **148**, 204305 (2018); <https://doi.org/10.1063/1.5028298>

[Calculations of positron binding and annihilation in polyatomic molecules](#)

The Journal of Chemical Physics **149**, 244305 (2018); <https://doi.org/10.1063/1.5055724>

[Formation of hot hydrogen atoms from superexcited states of acetylene](#)

The Journal of Chemical Physics **149**, 244302 (2018); <https://doi.org/10.1063/1.5058101>

Where in the **world** is AIP Publishing?
Find out where we are exhibiting next



Total cross section measurements for electron scattering from dichloromethane

A. I. Lozano,^{1,2} L. Álvarez,¹ F. Blanco,³ M. J. Brunger,⁴ and G. García^{1,5,a)}

¹*Instituto de Física Fundamental, CSIC, E-28006 Madrid, Spain*

²*Escuela de Doctorado de la UNED—Programa de Doctorado en Ciencias, 28015 Madrid, Spain*

³*Departamento de Física Atómica, Molecular y Nuclear, Universidad Complutense de Madrid, 28040 Madrid, Spain*

⁴*College of Science and Engineering, Flinders University, GPO Box 2100, Adelaide, SA 5001, Australia*

⁵*Centre for Medical Radiation Physics, University of Wollongong, Northfields Ave., Wollongong, NSW 2522, Australia*

(Received 10 November 2018; accepted 5 December 2018; published online 26 December 2018)

Using our magnetically confined electron transmission apparatus, we report the results of total cross sections (TCSs) for electron scattering from dichloromethane (CH_2Cl_2). The energy range of this study is 1–300 eV. Wherever possible, the present data are compared to earlier measured TCSs of Wan *et al.* [J. Chem. Phys. **94**, 1865 (1991)] and Karwasz *et al.* [Phys. Rev. A **59**, 1341 (1999)] and to the corresponding theoretical independent atom model with screening corrected additivity rule and interference term (IAM-SCAR+I) results of Krupa *et al.* [Phys. Rev. A **97**, 042702 (2018)] and a spherical complex optical potential formulation calculation of Naghma *et al.* [J. Electron Spectrosc. Relat. Phenom. **193**, 48 (2014)]. Within their respective uncertainties, the present TCS and those of Karwasz *et al.* are found to be in very good agreement over their common energy range. However, agreement with the results of Wan *et al.* is quite poor. The importance of the experimentally inherent ‘missing angle’ effect (see later) on the measured TCS is investigated and found to be significant at the lower energies studied. Indeed, when this effect is accounted for, agreement between our measured TCSs and the corrected IAM-SCAR+I+rotations calculation results are, for energies above about 3 eV, in good accord (to better than 8%). Finally, we observe two σ^* shape resonances, consistent with the earlier electron transmission spectroscopy results of Burrow *et al.* [J. Chem. Phys. **77**, 2699 (1982)], at about 2.8 eV and 4.4 eV incident electron energy, in our measured TCS. *Published by AIP Publishing.* <https://doi.org/10.1063/1.5080636>

I. INTRODUCTION

Total cross section (TCS) measurements have been undertaken since the genesis of electron–atom and electron–molecule collision experiments,¹ but in recent times, even though they can be typically measured to the highest precision,² they appear to have become a little undervalued by the scattering community. This largely stems from the fact that they cannot differentiate between the various scattering processes that occur in the collision interactions nor do they provide any angular information as to the scattering of the incident projectile. With increasing interest in modeling charged-particle transport phenomena,^{3–6} which requires a complete cross section database over an extended energy range,⁷ there has been renewed interest in measuring and calculating the total cross section for a given species of interest. This follows as the total cross section provides a crucial self-consistency check when one starts to form such a database for the simulations as the integral cross sections (ICSs) for all energetically open channels (e.g., elastic scattering, vibrational excitation,

ionisation, and so on) must add up, at a given incident electron energy, to the TCS.^{8–11}

With respect to the particular case of dichloromethane (CH_2Cl_2), there have been two recent electron impact studies^{12,13} which have detailed why *a priori* it is an interesting species to investigate. As a consequence, we do not repeat that information here. In addition, both those investigations^{12,13} provided excellent summaries of the currently available cross section data for electron scattering from CH_2Cl_2 . We therefore also do not repeat those details here, except to note the previous TCS experimental results of Wan *et al.*,¹⁴ for energies in the range 0.18–12 eV, and the data of Karwasz *et al.*,¹⁵ for energies in the range 75–4000 eV. From a theoretical perspective, we note results from a spherical complex optical potential (SCOP) formulation¹⁶ and an independent atom model with screening additivity rule and interference term approach (IAM-SCAR+I),¹² the latter also being extended to incorporate rotational excitation using a Born framework that is applicable to polar molecules like CH_2Cl_2 (IAM-SCAR+I+rotations).¹² Herein lie three of the main rationales for our investigation. Firstly, as Wan *et al.*¹⁴ and Karwasz *et al.*¹⁵ did not overlap in energy, we therefore seek to provide an independent assessment of their results. Secondly, we also seek to “fill in” the TCSs at the missing energies between the early

^{a)}Author to whom correspondence should be addressed: g.garcia@csic.es

experiments which thus opens up the possibility of forming a TCS database over a very wide energy regime. Finally, we aim to provide new data in order to further test the validity of the available theoretical cross sections.

The remainder of this short paper is structured as follows. In Sec. II, we describe our experimental approach, while in Sec. III, the present results and a discussion of those results are given. Finally, in Sec. IV, we provide some conclusions from the current investigation.

II. EXPERIMENTAL DETAILS

The present apparatus and our measurement techniques have been explained in detail previously,^{17–19} but nonetheless, to ensure this paper is largely self-contained, some of their more important facets are summarised here again. Our transmission-beam attenuation spectrometer consists of a linear electron beam that is confined by an intense (~ 0.1 T) axial magnetic field, which converts any scattering event into a kinetic energy loss in the forward direction (i.e., parallel to the applied magnetic field¹⁹). The primary electron beam, generated through thermionic emission from a tungsten filament, is cooled and confined in a magnetic molecular nitrogen (N_2) gas trap (GT), which reduces the initial energy spread (ΔE) of 500 meV down to about 200 meV (see Table I). Pulsed voltages, applied to the trap electrodes,¹⁹ produce a pulsed electron beam with a well-defined energy (and relatively narrow ΔE) to enter into the scattering cell. The scattering chamber (SC) is a 40 mm long gas cell, defined by two 1.5 mm diameter entrance and exit apertures, through which the pulsed electron beam passes when the CH_2Cl_2 pressure inside the chamber is varied from 0 to 2.5 mTorr (as measured by a MKS-Baratron 627B absolute capacitance manometer), with the upper limit being chosen to ensure multiple scattering effects are avoided. Note that before the CH_2Cl_2 vapour enters the SC, it is repeatedly degassed through the performance of freeze-pump-thaw cycles. Electrons emerging from the SC are analyzed in energy by a retarding potential analyser (RPA) and finally detected by a double microchannel plate electron multiplier operating in single counting mode. The total cross section ($TCS-\sigma_T$) is determined from the transmitted intensity, which follows the well-known Beer-Lambert attenuation law for ideal gases

$$\ln\left(\frac{I}{I_0}\right) = -L\sigma_T n = -\frac{L\sigma_T}{kT}p, \quad (1)$$

where I is the transmitted electron intensity, I_0 is the initial intensity, n is the CH_2Cl_2 gas density, L is the interaction region length (40 mm), k is Boltzmann's constant, T is the absolute temperature, and p is the CH_2Cl_2 gas pressure. T is derived from $T = \sqrt{T_c T_m}$, where T_c and T_m are, respectively, the temperature of the SC (as measured with a calibrated thermocouple) and the temperature of the Baratron manometer. Measurement conditions, data acquisition, and data analysis are monitored and controlled by a custom designed LabView (National Instruments) programme.

In our present investigation, the incident electron energy is calibrated using the well-known N_2 resonance feature^{2,20} at

~ 2.5 eV, and we believe it is accurate to better than ± 0.1 eV. Before undertaking the measurements with CH_2Cl_2 , we also checked the apparatus' performance by measuring the N_2 TCS between 1 and 300 eV. Very good agreement was found between our measurement and the earlier data of Szymthowski *et al.*²⁰ (to within 3%), thereby giving us confidence in our experimental procedures.

For each incident electron energy (E), attenuation measurements were repeated at least 5 times in order to ensure that the statistical uncertainties remained below 5%. Other random uncertainties are related to the temperature measurement ($\sim 1\%$ according to the manufacturer's data) and the numerical fitting procedure ($\sim 1\%$) associated with the analysis of the RPA cut-off curves.¹⁹ By combining these uncertainties, a total error limit of $\pm 6\%$ has been determined for the present TCSs. Systematic errors linked to the experimental configuration are those connected to the so-called "missing angles." Note that this is also an issue with a positron scattering apparatus that employs a confining magnetic field.²¹ Due to the magnetic field confinement, the energy width (or resolution) ΔE determines the angular resolution (or acceptance angle) $\Delta\theta$ of the detector from

$$\Delta\theta = \arcsin \sqrt{\frac{\Delta E}{E}}, \quad (2)$$

with the relevant values for ΔE (in eV) and $\Delta\theta$ (in degrees) of this study being listed in Table I. As detailed in Ref. 19, and also in the studies of Fuss *et al.*¹⁷ and Sanz *et al.*,¹⁸ the magnitude of this systematic error ($\sigma(\Delta\theta)$) can be evaluated from the available theoretical data (in this case, the IAM-SCAR+I+rotations results of Krupa *et al.*¹²) by integrating the calculated elastic and rotational differential cross sections (DCSs) over the "missing angles" via¹⁹

$$\sigma(\Delta\theta) = 2\pi \left[\int_0^{\Delta\theta} (DCS_{el} + DCS_{rot}) \sin \theta d\theta + \int_{180-\Delta\theta}^{180} (DCS_{el} + DCS_{rot}) \sin \theta d\theta \right], \quad (3)$$

where DCS_{el} and DCS_{rot} represent the elastic and rotational differential cross sections, respectively. This effect is particularly important for polar molecules such as CH_2Cl_2 , with the results from our present evaluation with Eq. (3) being given in Table I. In this case, we chose the IAM-SCAR+I+rotations theoretical results to evaluate Eq. (3), at each incident electron energy, simply because we had that data readily available to us across 1–300 eV. However, if we had chosen the Schwinger multichannel method implemented with pseudopotentials and employing the Born-closure method (SMCPP + BC) instead,¹² at energies between 1 and 20 eV where they are available, the results would be quantitatively similar to those already given in Table I. Finally, by subtracting the "missing angles" (or forward angles) cross section correction ($\sigma(\Delta\theta)$) from the TCS obtained from the IAM-SCAR+I+rotations calculation of Krupa *et al.*,¹² we generate the corrected theoretical TCS that is given in the last column of Table I. These are the theory data that most readily compare to our measured TCS (as given in column 2 of Table I).

TABLE I. Present total cross section data, with their random uncertainty, energy (ΔE), and angular ($\Delta\theta$) resolutions, for electron scattering from dichloromethane. Also shown is the magnitude of the systematic error due to the “missing angles” ($\sigma(\Delta\theta)$), estimated with the IAM-SCAR+I+rotations¹² calculations, and the corrected IAM-SCAR+I+rotations TCSs when that effect is accounted for.

<i>E</i> (eV)	Experiment					Theory	
	TCS ($\times 10^{-16}$ cm ²)	Random uncertainty ($\times 10^{-16}$ cm ²)	ΔE (eV)	$\Delta\theta$ (deg)	“Missing angle” corrections ($\sigma(\Delta\theta)$) ($\times 10^{-16}$ cm ²)	IAM-SCAR+I+ rotations ¹² – “missing angle” corrections ($\times 10^{-16}$ cm ²)	
1.0	46.4	1.2	0.2	26.6	78.1	57.1	
1.2	43.6	1.7	0.2	24.1			
1.4	42.3	1.4	0.2	22.2			
1.6	40.5	1.2	0.2	20.7			
1.8	38.6	0.7	0.2	19.5			
2.0	39.4	1.3	0.2	18.4	40.5	50.2	
2.2	40.0	1.4	0.2	17.5			
2.4	42.0	0.6	0.2	16.8			
2.6	44.5	1.2	0.2	16.1			
2.8	45.5	0.7	0.2	15.5			
3.0	44.4	0.7	0.2	15.0	28.3	46.5	
3.2	43.1	0.2	0.2	14.5			
3.4	42.6	1.1	0.2	14.0			
3.6	43.2	1.3	0.2	13.6			
3.8	43.7	1.8	0.2	13.3			
4.0	44.4	1.8	0.2	12.9	22.2	45.6	
4.2	45.7	1.4	0.2	12.6			
4.4	45.9	1.4	0.2	12.3			
4.6	46.4	1.7	0.2	12.0			
4.8	45.4	0.7	0.2	11.8			
5.0	44.5	1.6	0.2	11.5	18.7	45.4	
5.3	44.2	0.4	0.2	11.2			
5.5	44.9	0.6	0.2	11.0			
5.8	45.7	1.1	0.2	10.7			
6.0	46.0	1.3	0.2	10.5			
6.5	46.4	1.8	0.2	10.1			
7.0	46.9	0.9	0.2	9.7	14.4	47.8	
7.5	47.7	1.0	0.2	9.4			
7.7	48.5	0.8	0.2	9.3			
8.0	49.9	1.9	0.2	9.1			
8.5	50.9	0.5	0.2	8.8			
9.0	51.2	1.1	0.2	8.6			
9.5	52.3	1.2	0.2	8.3			
10	52.8	0.5	0.2	8.1	11.1	52.2	
11	52.7	0.5	0.2	7.7			
12	52.6	0.9	0.2	7.4			
13	52.4	1.7	0.2	7.1			
14	51.0	0.8	0.2	6.9			
15	49.6	1.2	0.2	6.6	8.3	51.3	
16	48.0	0.9	0.2	6.4			
17	47.1	1.0	0.2	6.2			
18	46.5	1.4	0.2	6.1			
19	45.1	1.1	0.2	5.9			
20	44.3	1.8	0.2	5.7	6.3	46.9	
22	43.0	0.9	0.2	5.5			
25	41.9	1.3	0.2	5.1			
28	40.8	1.2	0.2	4.8			
30	40.1	0.8	0.2	4.7	4.5	39.5	
33	39.1	1.6	0.2	4.5			
35	37.9	1.2	0.22	4.5			
38	36.6	0.7	0.22	4.4			
40	35.5	1.1	0.22	4.3	3.1	35.0	
45	33.8	1.0	0.23	4.1			
50	32.3	1.4	0.22	3.8	2.8	31.4	

TABLE I. (Continued.)

E (eV)	Experiment				Theory	
	TCS ($\times 10^{-16}$ cm 2)	Random uncertainty ($\times 10^{-16}$ cm 2)	ΔE (eV)	$\Delta\theta$ (deg)	“Missing angle” corrections ($\sigma(\Delta\theta)$) ($\times 10^{-16}$ cm 2)	IAM-SCAR+I+ rotations ¹² – “missing angle” corrections ($\times 10^{-16}$ cm 2)
55	31.0	0.5	0.23	3.7		
60	29.95	0.9	0.20	3.3		
70	28.3	1.2	0.25	3.4	1.9	27.2
80	26.4	0.5	0.25	3.2		
90	24.5	0.9	0.25	3.0		
100	23.3	0.4	0.25	2.9	1.6	23.0
120	20.8	0.3	0.25	2.6		
150	18.9	0.6	0.25	2.3	0.9	19.2
200	15.9	0.4	0.27	2.1	0.8	16.6
250	13.6	0.2	0.30	2.0		
300	12.4	0.11	0.35	2.0	0.7	13.4

III. RESULTS AND DISCUSSION

In Table I, we list the present experimental TCS data, with those results additionally being plotted in Fig. 1. Also plotted in Fig. 1 are the TCS results from the previous measurements of Wan *et al.*¹⁴ and Karwasz *et al.*,¹⁵ along with theoretical IAM-SCAR+I and IAM-SCAR+I+rotations total cross sections of Krupa *et al.*¹² and an SCOP result of

Naghma *et al.*¹⁶ The corrected, for the “missing angle” effect, IAM-SCAR+I+rotations TCSs are also given in this figure. Finally, some recent experimental elastic ICSs of Hlousek *et al.*¹³ are also included. We note that experimental elastic ICSs, over a more restricted energy range, were also reported in the work of Krupa *et al.*¹² Those ICSs were derived from their elastic DCSs, whose angular distributions appear to be uncorrected for the “effective path length correction factor.”^{2,22} The effective path length correction factor, which is energy dependent, results from the different target electron/molecular beam overlap profiles as the scattered electron detector is rotated about 0° scattering angle²² and is particularly important at the more forward scattering angles. As the angular distributions of Krupa *et al.*¹² were not corrected for this, the ICSs derived from them are possibly unreliable and this is why they are not plotted here. Note that the elastic DCSs in the work of Hlousek *et al.*¹³ were all measured using a variant of the relative flow technique,^{23–25} which, if correctly applied, cancels out any possible effective path length correction factor. We therefore believe that the elastic DCSs of Hlousek *et al.*¹³ are credible so that their ICSs are also sound and hence plotted in Fig. 1.

Considering Fig. 1 in more detail, we find that our measured TCS exhibits two resonance structures at about 2.8 eV and 4.4 eV. Resonances in electron scattering from CH_2Cl_2 were first identified in the electron transmission spectroscopy work of Burrow *et al.*,²⁶ who assigned their origin as being σ shape resonances. While none of the present TCS theoretical computations exhibit any resonance structure (see Fig. 1), which is to be expected given their independent atom formulation, elastic ICS calculations of Krupa *et al.*¹² and Hlousek *et al.*¹³ both do. In the case of the most physical Schwinger Multichannel (SMC) computation,¹² σ^* shape resonances of A_1 -symmetry and B_2 -symmetry were identified at 1.5 eV and 3.6 eV. For the theoretical results reported by Hlousek *et al.*,¹³ the B_2 -symmetry peak was determined to be at around 5 eV. While there is a slight mismatch between the experimental and theoretical resonance energy positions, this is by no means unusual and depends upon things such as the type of

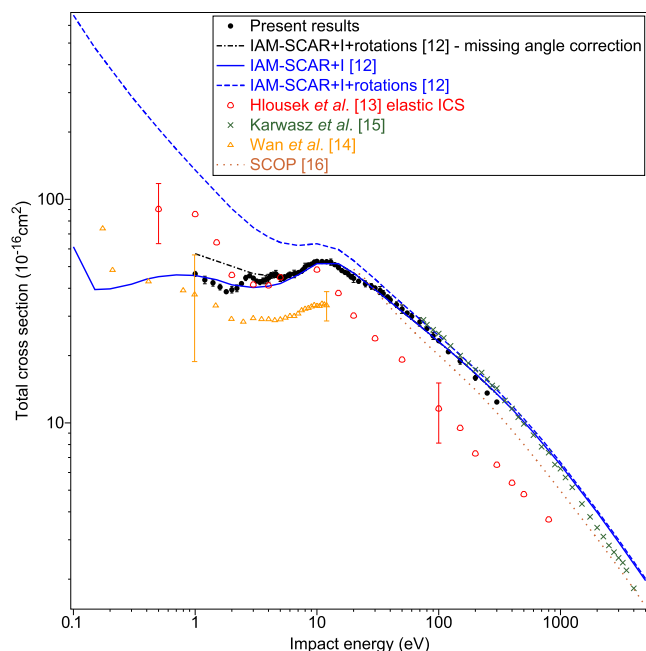


FIG. 1. Total cross sections ($\times 10^{-16}$ cm 2) for electron scattering from CH_2Cl_2 . The present data (black filled circles) are compared against earlier measurements of Wan *et al.*¹⁴ (orange open triangles) and Karwasz *et al.*¹⁵ (green crosses) and theoretical IAM-SCAR+I (blue solid curve)¹² and IAM-SCAR+I+rotations (blue short dashed curve)¹² and SCOP (brown dotted curve)¹⁶ results. The IAM-SCAR+I+rotations result when corrected for the “missing angle” effect (black dotted-dashed curve)¹⁹ and the measured elastic ICSs of Hlousek *et al.*¹³ (red open circles) are also shown. Note that the uncertainties on the present data are statistical only. See also the legend on the figure.

theoretical approach employed and whether it is at the static exchange (SE) or static exchange plus polarisation (SEP) levels and indeed on the size of the basis states that can be realistically employed in the scattering computations. We therefore believe that the resonance structures we observe in Fig. 1 are physical and can be attributed to the filling of unoccupied C–Cl σ^* -orbitals.²⁶

We have previously referred to the importance of the “missing angle” effect, and by using the IAM-SCAR+I+ rotations calculations of Krupa *et al.*¹² and Eqs. (2) and (3), we can quantify that effect. The results of this process ($\sigma(\Delta\theta)$) are summarised in Table I, where we can see that the effect is particularly significant at the lower energies. Specifically, the “missing angle” correction is some 168% of the measured TCS at 1 eV, some 21% of the measured TCS at 10 eV, 7% of the measured TCS at 70 eV, and 5% of the measured TCS at 300 eV. Therefore, above about 70 eV, the “missing angle” correction is of the order of the overall uncertainties we cite on our measured TCS. When this correction is applied to the IAM-SCAR+I+rotations TCSs (see the last column of Table I), at each energy, excellent agreement is now found (to better than 8%) between the corrected theory and our measured TCS above about 3 eV (see Fig. 1). It is also apparent from Fig. 1 that, over their common energy range and to within the stated uncertainties, the present TCS data and the earlier measurements of Karwasz *et al.*¹⁵ are in very good accord. Agreement with the results of Wan *et al.*¹⁴ is, however, quite marginal although the qualitative shapes of both TCSs are rather similar. The reason for this mismatch in the absolute value between the results of Wan *et al.* and our results is not immediately clear to us. While Wan *et al.*¹⁴ also used a magnetic confinement linear transmission apparatus, their energy resolution ($\Delta E \sim 0.05$ eV) and thus angular resolution ($\Delta\theta$) were superior to the present resolution, and so their “missing angle” correction would be less significant. Hence you might have *a priori* expected their measured TCS to show a higher magnitude than the present! Nonetheless there are a couple of possible factors that might explain, at least in part, this apparent paradox. First, the confining B-field used by Wan *et al.*¹⁴ (0.007 T) was much weaker than that used in the present and second the technology that underpins modern capacitance manometers, in terms of the accuracy of the pressure reading and their stability, is far superior today than they were back in 1991. In principle, the elastic ICSs should always have a somewhat lower magnitude than the total cross sections as the TCSs incorporate all open channels (including the elastic channel) at a given energy. This is precisely what we found in Fig. 1 above about 10 eV, when the measured elastic ICSs of Hlousek *et al.*¹³ are compared to the present TCSs. Note that 10 eV roughly coincides with the ionisation energy threshold for CH₂Cl₂²⁷ so that the observed difference in magnitude between the elastic ICS and our measured TCS can largely be ascribed to the total ionisation cross section of dichloromethane.²⁷ Below 10 eV, however, there appears to be something of a contradiction as the elastic ICSs¹³ are either of the same magnitude as our TCS or are significantly greater in magnitude than our TCS (see Fig. 1). This apparent paradox at these lower energies can once again be explained by the “missing angle” effect. If our measured TCSs were to be corrected for the “missing angle” effect, to give the physical

TCSs, then their magnitude would increase significantly and this apparent contradiction, particularly when allowance was made for the $\pm 30\%$ errors on the elastic ICSs, would certainly disappear.

IV. CONCLUSIONS

We have reported absolute total cross section data for electrons scattering from the polar molecule dichloromethane. The present results were found to be in very good agreement with the earlier measurements of Karwasz *et al.*,¹⁵ over their common energy range. This raises the possibility that a recommended TCS dataset might be constructed for electron energies between 1 and 4000 eV, provided that a “missing angle” correction is applied to the lower energy data. Using the IAM-SCAR+I+rotations theoretical results of Krupa *et al.*¹² and Eqs. (2) and (3), we were able to quantify the “missing angle” correction and found it to be a significant effect here at the lower energies. Indeed once accounted for, excellent agreement (to better than 8%) was observed between the corrected IAM-SCAR+I+rotations TCS and our measured TCS for energies above about 3 eV. The importance of the “missing angle” correction when using a linear transmission apparatus with a confining magnetic field and polar molecules has also been observed by us in some of our previous investigations.^{17,28} Finally, we observed two quite strong resonance features, at energies of ~ 2.8 eV and 4.4 eV, in our measured TCS. Those features, consistent with the earlier electron transmission spectroscopy work of Burrow *et al.*²⁶ and elastic ICS calculations in the studies of Krupa *et al.*¹² and Hlousek *et al.*,¹³ were assigned to originate from the temporary capture of electrons into unoccupied C–Cl σ^* -orbitals of CH₂Cl₂.

ACKNOWLEDGMENTS

This work was financially supported, in part, by the Spanish Ministerio de Ciencia, Innovacion y Universidades (Project No. FIS2016-80440) and the Australia Research Council (Project Nos. DP160102787 and DP180101655). We thank Dr. L. Campbell for his help with some aspects of this study and Professor M. Khakoo for providing us with a preprint of his paper.

¹M. J. Brunger and S. J. Buckman, *Nucleus* **34**, 201 (1997).

²M. J. Brunger and S. J. Buckman, *Phys. Rep.* **357**, 215 (2002).

³A. I. Lozano, K. Krupa, F. Ferreira da Silva, P. Limão-Vieira, F. Blanco, A. Muñoz, D. B. Jones, M. J. Brunger, and G. García, *Eur. Phys. J. D* **71**, 226 (2017).

⁴A. I. Lozano, J. C. Oller, D. B. Jones, R. F. da Costa, M. T. do N. Varella, M. H. F. Bettega, F. Ferreira da Silva, P. Limão-Vieira, M. A. P. Lima, R. D. White, M. J. Brunger, F. Blanco, A. Muñoz, and G. García, *Phys. Chem. Chem. Phys.* **20**, 22368 (2018).

⁵M. J. E. Casey, J. de Urquijo, L. N. Serkovic Loli, D. G. Cocks, G. J. Boyle, D. B. Jones, M. J. Brunger, and R. D. White, *J. Chem. Phys.* **147**, 195103 (2017).

⁶R. D. White, D. Cocks, G. Boyle, M. Casey, N. Garland, D. Konovalov, B. Philippa, P. Stokes, J. de Urquijo, O. González-Magaña, R. P. McEachran, S. J. Buckman, M. J. Brunger, G. García, S. Dujko, and Z. Lj. Petrovic, *Plasma Sources Sci. Technol.* **27**, 053001 (2018).

⁷H. Tanaka, M. J. Brunger, L. Campbell, H. Kato, M. Hoshino, and A. R. P. Rau, *Rev. Mod. Phys.* **88**, 025004 (2016).

⁸M. J. Brunger, *Int. Rev. Phys. Chem.* **36**, 333 (2017).

- ⁹M. A. Ridenti, J. A. Filho, M. J. Brunger, R. F. da Costa, M. T. do N. Varella, M. H. F. Bettega, and M. A. P. Lima, *Eur. Phys. J. D* **70**, 161 (2016).
- ¹⁰M. J. Brunger, K. Ratnavelu, S. J. Buckman, D. B. Jones, A. Muñoz, F. Blanco, and G. Garcia, *Eur. Phys. J. D* **70**, 46 (2016).
- ¹¹M. C. Fuss, L. Ellis-Gibblings, D. B. Jones, M. J. Brunger, F. Blanco, A. Muñoz, P. Limão-Vieira, and G. García, *J. Appl. Phys.* **117**, 214701 (2015).
- ¹²K. Krupa, E. Lange, F. Blanco, A. S. Barbosa, D. F. Pastega, S. d'A. Sanchez, M. H. F. Bettega, G. García, P. Limão-Vieira, and F. Ferreira da Silva, *Phys. Rev. A* **97**, 042702 (2018).
- ¹³B. A. Hlousek, M. F. Martin, M. Zawadzki, M. A. Khakoo, L. E. Machado, R. R. Lucchese, V. A. S. da Mala, I. Iga, M.-T. Less, and M. G. P. Homem, *J. Phys. B* **52**, 025204 (2019).
- ¹⁴H.-X. Wan, J. H. Moore, and J. A. Tossell, *J. Chem. Phys.* **94**, 1868 (1991).
- ¹⁵G. P. Karwasz, R. S. Brusa, A. Piazza, and A. Zecca, *Phys. Rev. A* **59**, 1341 (1999).
- ¹⁶R. Naghma, D. Gupta, and B. Antony, *J. Electron Spectrosc. Relat. Phenom.* **193**, 48 (2014).
- ¹⁷M. C. Fuss, A. G. Sanz, F. Blanco, J. C. Oller, P. Limão-Vieira, M. J. Brunger, and G. García, *Phys. Rev. A* **88**, 042702 (2013).
- ¹⁸A. G. Sanz, M. C. Fuss, F. Blanco, J. D. Gorfinkiel, D. Almeida, F. Ferreira da Silva, P. Limão-Vieira, M. J. Brunger, and G. García, *J. Chem. Phys.* **139**, 184310 (2013).
- ¹⁹A. I. Lozano, J. C. Oller, K. Krupa, P. Limão-Vieira, F. Blanco, A. Muñoz, R. Colmenares, and G. García, *Rev. Sci. Instrum.* **89**, 063105 (2018).
- ²⁰C. Szmythowski, K. Maciag, and G. Karwasz, *Phys. Scr.* **54**, 271 (1996).
- ²¹M. J. Brunger, S. J. Buckman, and K. Ratnavelu, *J. Phys. Chem. Ref. Data* **46**, 023102 (2017).
- ²²R. T. Brinkmann and S. Trajmar, *J. Phys. E* **14**, 245 (1981).
- ²³J. C. Nickel, P. W. Zetner, G. Shen, and S. Trajmar, *J. Phys. E* **22**, 730 (1989).
- ²⁴L. R. Hargreaves, J. R. Francis-Staite, T. M. Maddern, M. J. Brunger, and S. J. Buckman, *Meas. Sci. Technol.* **18**, 2783 (2007).
- ²⁵T. M. Maddern, L. R. Hargreaves, M. Bolorizadeh, M. J. Brunger, and S. J. Buckman, *Meas. Sci. Technol.* **19**, 085801 (2008).
- ²⁶P. D. Burrow, A. Modelli, N. S. Chiu, and K. D. Jordan, *J. Chem. Phys.* **77**, 2699 (1982).
- ²⁷M. Bart, P. W. Harland, J. E. Hudson, and C. Vallance, *Phys. Chem. Chem. Phys.* **3**, 800 (2001).
- ²⁸A. I. Lozano, F. Ferreira da Silva, F. Blanco, P. Limão-Vieira, and G. García, *Chem. Phys. Lett.* **706**, 533 (2018).